

This is a repository copy of *The crystal structure of superoxide dismutase from Plasmodium falciparum*.

White Rose Research Online URL for this paper:

<https://eprints.whiterose.ac.uk/id/eprint/1873/>

Article:

Boucher, Ian W., Brzozowski, Andrzej M. orcid.org/0000-0001-7426-8948, Brannigan, James A. orcid.org/0000-0001-6597-8972 et al. (4 more authors) (2006) The crystal structure of superoxide dismutase from Plasmodium falciparum. BMC Structural Biology. -. ISSN 1472-6807

<https://doi.org/10.1186/1472-6807-6-20>

Reuse

Items deposited in White Rose Research Online are protected by copyright, with all rights reserved unless indicated otherwise. They may be downloaded and/or printed for private study, or other acts as permitted by national copyright laws. The publisher or other rights holders may allow further reproduction and re-use of the full text version. This is indicated by the licence information on the White Rose Research Online record for the item.

Takedown

If you consider content in White Rose Research Online to be in breach of UK law, please notify us by emailing eprints@whiterose.ac.uk including the URL of the record and the reason for the withdrawal request.

promoting access to White Rose research papers



Universities of Leeds, Sheffield and York
<http://eprints.whiterose.ac.uk/>

White Rose Research Online URL for this paper:
<http://eprints.whiterose.ac.uk/1873/>

Published paper

Boucher, I.W., Brzozowski, A.M., Brannigan, J.A., Schnick, C., Smith, D.J., Kyes, S.A. and Wilkinson, A.J. (2006) *The crystal structure of super-oxide dismutase from Plasmodium falciparum*, BMC Structural Biology, Volume 6 (20).

Research article

Open Access

The crystal structure of superoxide dismutase from *Plasmodium falciparum*

Ian W Boucher¹, Andrzej M Brzozowski¹, James A Brannigan*¹,
Claudia Schnick¹, Derek J Smith^{1,3}, Sue A Kyes² and Anthony J Wilkinson¹

Address: ¹Structural Biology Laboratory, Department of Chemistry, University of York, York YO10 5YW, UK, ²Molecular Parasitology Group, Weatherall Institute of Molecular Medicine, John Radcliffe Hospital, Headington, Oxford OX3 9DS, UK and ³Bioinformatics Institute, 30 Biopolis St., Singapore 138671, Singapore

Email: Ian W Boucher - boucher@ysbl.york.ac.uk; Andrzej M Brzozowski - marek@ysbl.york.ac.uk; James A Brannigan* - jab@ysbl.york.ac.uk; Claudia Schnick - schnick@ysbl.york.ac.uk; Derek J Smith - smith@bii.a-star.edu.sg; Sue A Kyes - Skyes@hammer.imm.ox.ac.uk; Anthony J Wilkinson - ajw@ysbl.york.ac.uk

* Corresponding author

Published: 04 October 2006

Received: 08 June 2006

BMC Structural Biology 2006, 6:20 doi:10.1186/1472-6807-6-20

Accepted: 04 October 2006

This article is available from: <http://www.biomedcentral.com/1472-6807/6/20>

© 2006 Boucher et al; licensee BioMed Central Ltd.

This is an Open Access article distributed under the terms of the Creative Commons Attribution License (<http://creativecommons.org/licenses/by/2.0>), which permits unrestricted use, distribution, and reproduction in any medium, provided the original work is properly cited.

Abstract

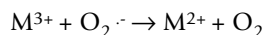
Background: Superoxide dismutases (SODs) are important enzymes in defence against oxidative stress. In *Plasmodium falciparum*, they may be expected to have special significance since part of the parasite life cycle is spent in red blood cells where the formation of reactive oxygen species is likely to be promoted by the products of haemoglobin breakdown. Thus, inhibitors of *P. falciparum* SODs have potential as anti-malarial compounds. As a step towards their development we have determined the crystal structure of the parasite's cytosolic iron superoxide dismutase.

Results: The cytosolic iron superoxide dismutase from *P. falciparum* (PfFeSOD) has been overexpressed in *E. coli* in a catalytically active form. Its crystal structure has been solved by molecular replacement and refined against data extending to 2.5 Å resolution. The structure reveals a two-domain organisation and an iron centre in which the metal is coordinated by three histidines, an aspartate and a solvent molecule. Consistent with ultracentrifugation analysis the enzyme is a dimer in which a hydrogen bonding lattice links the two active centres.

Conclusion: The tertiary structure of PfFeSOD is very similar to those of a number of other iron- and manganese-dependent superoxide dismutases, moreover the active site residues are conserved suggesting a common mechanism of action. Comparison of the dimer interfaces of PfFeSOD with the human manganese-dependent superoxide dismutase reveals a number of differences, which may underpin the design of parasite-selective superoxide dismutase inhibitors.

Background

Superoxide dismutases (SODs) are crucial enzymes in both eukaryotes and prokaryotes. They catalyse the dismutation of the superoxide radical to hydrogen peroxide and dioxygen according to the two-step reaction as follows:



where M denotes a metal ion which interconverts between oxidised and reduced states. The superoxide radical $O_2^{\cdot -}$ is

formed in cells as a result of both enzymatic and spontaneous oxidation reactions. The superoxide radical is toxic to living cells as it oxidises and degrades biological molecules such as lipids and proteins [1].

For many years it was thought that malaria parasites had no requirement for an endogenous superoxide dismutase and merely exploited the activity of the host's enzyme in the red blood cell [2]. However, in 1996 a *Plasmodium falciparum* iron-dependent SOD (*PfFeSOD*) was identified in parasites isolated from infected blood cells [3]. Malaria parasites are particularly prone to oxidative damage in the intra-erythrocytic stage of their lifecycle. This is because an important source of amino acids for the parasite is red blood cell haemoglobin. Haemoglobin degradation produces free haem groups leading to oxidation of the iron from the ferrous (Fe^{2+}) to the ferric (Fe^{3+}) state. This oxidation liberates electrons, which promote the formation of reactive oxygen intermediates, including superoxide. The *PfFeSOD* gene is expressed at its highest level during this stage of the parasite life cycle [4].

SODs are classified according to their metal cofactors. Eukaryotic cells are generally served by a cytosolic Cu/ZnSOD and an evolutionarily unrelated mitochondrial MnSOD. Some eukaryotes also contain a SOD containing a single Fe atom. Bacterial cells feature single metal-centred SODs in which the metal can be either manganese or iron. The FeSODs and the MnSODs exhibit recognisable similarities in their sequences, they have a common α/β tertiary structure and they use the same residues to coordinate the metal [5]. These are quite distinct from the two-metal Cu/ZnSODs, which have a Greek key β -barrel fold [6]. The MnSODs of eukaryotic origin are distinguishable from those of prokaryotic sources on the basis of their quaternary structure; the former are tetramers while the latter are dimers. Small sequence differences distinguish the Mn- and FeSODs [7]. Biochemically, FeSODs are more sensitive to inhibition by azide [8] and have a greater susceptibility to inactivation by hydrogen peroxide, than MnSODs. Iron and manganese superoxide dismutases can bind either metal cofactor. However, most are only functional with their cognate metal co-factor bound. Some enzymes however, maintain activity with either Fe or Mn bound and are termed cambialistic [9].

In 2002, an electron paramagnetic resonance and modelling study of SOD from *P. falciparum* showed it was, as expected, an iron-dependent dimer [10]. The fact that it is an FeSOD and distinct from human tetrameric Mn and Cu/ZnSODs raises the possibility of its exploitation as an anti-malarial drug target [11] and indeed inhibitors of *PfFeSOD* have been identified [12]. This study presents an X-ray crystal structure of *P. falciparum* FeSOD solved at a resolution of 2.5 Å.

Results

Protein characterization

Purified *PfFeSOD* was resolved by electrophoresis for 3 hours at 100 V in a 10% native polyacrylamide gel. The gel was soaked in riboflavin and NADPH to generate superoxide radicals, and stained by Nitro Blue Tetrazolium (NBT) dye. NBT reacts with superoxide to form a blue precipitate when fixed in a gel. Any regions on the gel that exhibit SOD activity will therefore be white against a blue background. A clear white band coincident with the *PfFeSOD* protein indicated that the protein was active. Analytical ultracentrifugation (AUC) sedimentation equilibrium experiments estimated the molecular weight of the protein to be $47,400 \pm 700$ Da. Since the calculated molecular weight of the monomer is 23,799 Da, this indicates that *PfFeSOD* is a dimer, consistent with previously characterised FeSODs, which are either dimers or tetramers.

Overall structure

The crystal structure of *PfFeSOD* has been solved and refined against data extending to 2.5 Å spacing. The refined model consists of two polypeptide chains, A and B, which are related by a non-crystallographic two-fold axis of symmetry, together with two iron ions and 140 solvent water molecules. The electron density maps are contiguous from residue 1 to residue 197 of both chains. The C-terminal *PfFeSOD* residue (Lys¹⁹⁸), together with the eight residues of the C-terminal tag are not observed in the electron density maps. Details of the refinement statistics are given in Table 1. There is a solitary outlier in the Ramachandran plot at residue Lys⁴³ in the B chain, which occurs in a partially ordered surface loop. The Ser¹⁵-Pro¹⁶ peptide bond in both chains is in the *cis* conformation.

The overall structure is similar to those of previously solved iron superoxide dismutases, consisting of an amino terminal α -helical domain linked to a carboxy terminal α/β domain. The first eleven residues have an extended structure and are involved in crystal packing. The next 70 residues form two long anti-parallel α -helices ($\alpha 1$ and $\alpha 3$) connected by a meandering loop containing a third helix, $\alpha 2$. In both subunits, helix $\alpha 1$ has a noticeable kink at the conserved Lys²⁹ residue, a feature that has been noted before [13]. This domain is connected via an extended loop to the α/β domain (Figure 2A), which comprises a three-stranded anti-parallel β -pleated sheet (strand order $\beta 3$ - $\beta 1$ - $\beta 2$) surrounded by four α -helices. Superposition of equivalent C α atoms of chain A and chain B of *PfFeSOD* gives a positional root mean squared deviation (rms Δ) of 0.3 Å. The *PfFeSOD* structure superposes onto the molecular replacement model, *E. coli* FeSOD, with an rms Δ of 0.55 Å over all equivalent C α atoms.

Table 1: Data collection and refinement statistics

<i>Data collection</i>	
X-ray source	ESRF Beamline ID29
Wavelength (Å)	0.976000
Collection Temperature (K)	100
Resolution range (Å)	25.00 – 2.52
Space group	$P2_12_12_1$
Unit-cell parameters (Å)	$a = 55.94, b = 78.91, c = 90.62$
Matthews coefficient/solvent content (%)	2.2/43.0
Number of unique reflections, overall/outer shell ^a	13247 (843)
Completeness (%), overall/outer shell ^a	98.8 (100)
Redundancy, overall/outer shell ^a	4.1 (4.2)
$I/\sigma(I)$, overall/outer shell ^a	17.3 (6.2)
R_{merge}^b (%), overall/outer shell ^a	8.3 (29.7)
<i>Refinement and model statistics</i>	
R-factor ^c	0.187 (0.224)
R-free ^d	0.263 (0.338)
Molecules/asymmetric unit	2
Number of protein non hydrogen atoms	3345
Number of water molecules	140
Rms deviation from target ^e	
Bond lengths (Å)	0.014
Bond angles (°)	1.453
Average B-factor (Å ²)	28.10
Ramachandran plot ^f	90.3/8.6/0.6/0.6

^a Figures in parentheses concern the outer shell and corresponds to 2.582–2.520 Å.

^b $R_{\text{merge}} = \frac{\sum_{hkl} \sum_i |I_i - \langle I \rangle|}{\sum_{hkl} \sum_i \langle I \rangle}$ where I_i is the intensity of the i th measurement of a reflection with indexes hkl and $\langle I \rangle$ is the statistically weighted average reflection intensity.

^c $R\text{-factor} = \frac{\sum ||F_o| - |F_c||}{\sum |F_o|}$ where F_o and F_c are the observed and calculated structure factor amplitudes, respectively.

^d R-free is the R-factor calculated with 5 % of the reflections chosen at random and omitted from refinement.

^e Root-mean-square deviation of bond lengths or bond angles from ideal geometry.

^f Percentage of residues in most favoured/additionally allowed/generously allowed/disallowed regions of the Ramachandran plot, according to PROCHECK.

Structural comparisons and dimer interface

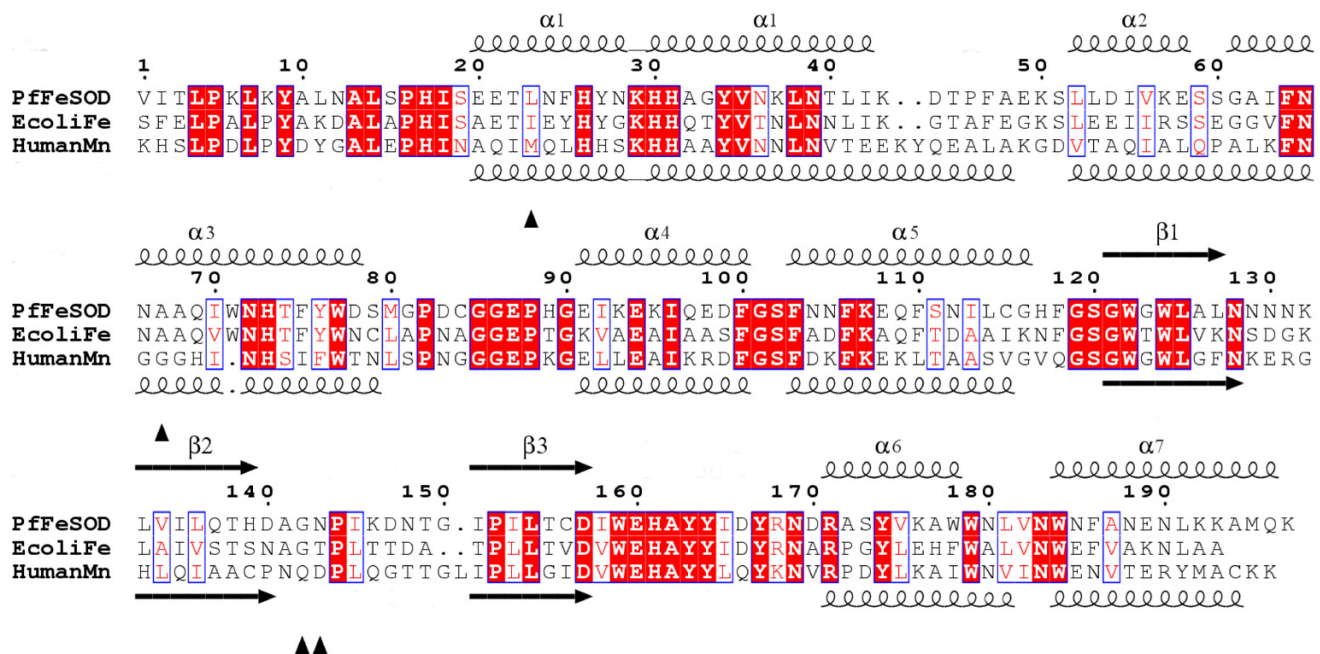
The tertiary structure is very similar to that of a number of other Fe- or Mn-dependent SOD enzymes. Of particular interest is comparison with the tetrameric MnSOD found in human mitochondria. Subtle differences in the structures may allow the design of inhibitors to block the activity of FeSOD selectively without affecting the MnSOD. The arrangement of the active site residues is well conserved between the Fe and MnSODs; the only significant difference in main chain conformation arises in the loop connecting $\alpha 1$ and $\alpha 3$, which is remote from the active site and the dimer interface.

As is typical of SOD proteins, only a relatively small accessible surface area (9.7 %) becomes buried in the dimer interface. The main contributions to the dimer interface arise from helix $\alpha 1$, the loop that connects $\alpha 5$ to $\beta 1$ and the loop connecting $\beta 3$ to $\alpha 6$. 41% of the atoms forming the dimer interface are polar, while 59% are non-polar. There are five bridging water molecules within the dimer interface. There is an interesting pair of adjacent charge-

charge interactions between the carboxylates of the Asp¹⁴⁰ residues and the side chain imidazoles of His¹³⁹. Perhaps associated with this, the dihedral angles of residue Asp¹⁴⁰ appear in a generously allowed location on the Ramachandran plot. These residues lie on what would be a classical β -turn were it not for the fact that residue 141 is an alanine rather than a glycine. All of the dimer stabilising interactions in the *E. coli* enzyme are conserved in PfFeSOD. Such high conservation of the dimer interface reflects the importance of dimerisation to the activity of dismutases.

Active site of *P. falciparum* FeSOD

The metal ion in both subunits of the enzyme is five-coordinate. Three bonds arise from coordination with histidine N $\epsilon 2$ atoms of residues His²⁶ (mean Fe-N $\epsilon 2$ distance 2.2 Å), His⁷³ (2.1 Å) and His¹⁶¹ (2.0 Å). A further bond is between the metal and the O $\delta 2$ atom of Asp¹⁵⁷ (mean Fe-O $\delta 2$ distance 1.9 Å). The fifth coordination position is an oxygen atom from either a water molecule or a hydroxide species (mean Fe-O distance 2.1 Å). The coordination

**Figure 1**

Sequence alignment of FeSOD from *P. falciparum* and *E. coli* and MnSOD from the human mitochondrion. Identical residues are highlighted with a red background and similar residues are boxed. P. falciparum FeSOD (top) and MnSOD (PDB code 1n0j [36] bottom) secondary structure elements are indicated. Residues predicted to be specific to MnSOD sequences [37] are marked with a triangle. Note the similarity of secondary structure between the two types of SOD. The longer helices in the N-terminal domain of MnSOD contribute to tetramer formation. The figure was made using ESPript [38].

geometry is trigonal bipyramidal, with His⁷³, His¹⁶¹ and Asp¹⁵⁷ providing the equatorial ligands and with His²⁶ and the hydroxide or water oxygen atom forming the axial ligands.

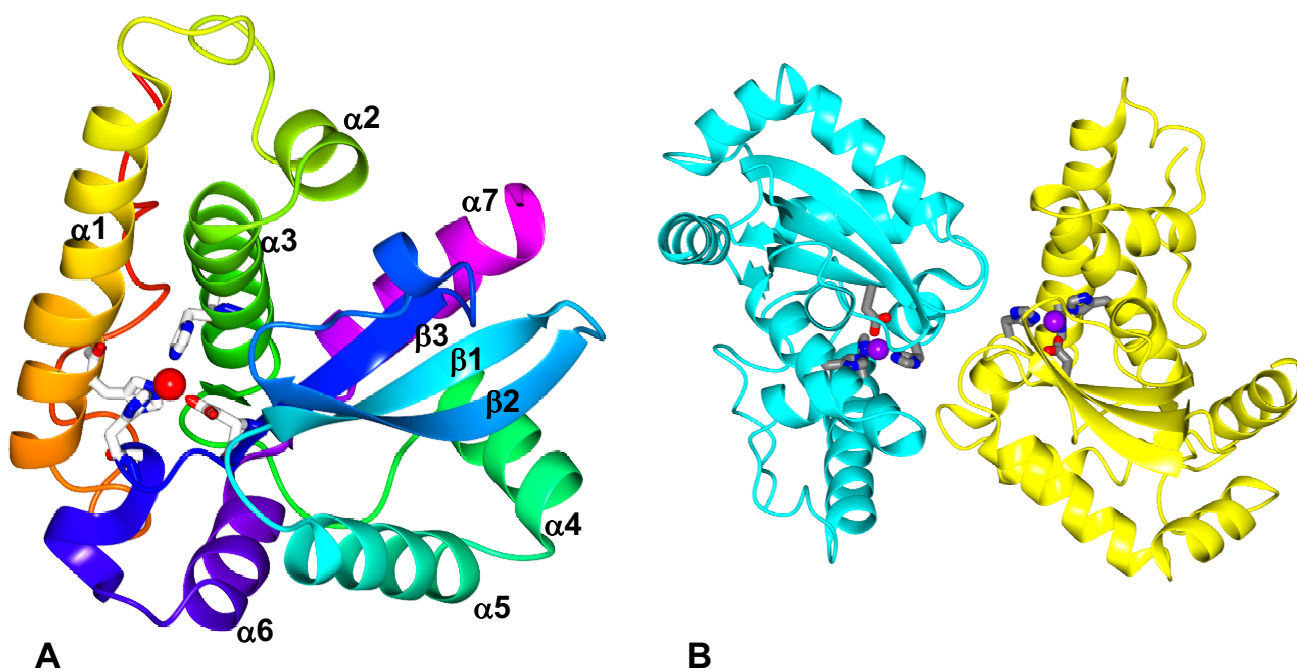
The area around the active site is fairly hydrophobic with two tryptophan residues (122 and 159) 5.4 Å and 6.1 Å from the metal, respectively. Trp¹²² forms a hydrogen bond to Gln⁶⁹, which in turn forms a hydrogen bond with the hydroxyl group of Tyr³⁴. Tyr³⁴ is also hydrogen bonded via a water molecule to His³⁰, which is bonded to Tyr¹³⁴ from the other subunit. This classical hydrogen-bonding network in superoxide dismutases may allow communication between the two metal sites [13]. In the B chain however, we note that the Gln⁶⁹ Nδ to Tyr³⁴-OH distance is longer (3.6 Å), perhaps due to coordinate error at this resolution. The spatial arrangement of the residues in the active site is otherwise identical to those of other Fe-dependent superoxide dismutases whose structures are known, consistent with the notion that structure and mechanism are highly conserved in this enzyme class.

A second line of communication between the active sites is afforded by the intermolecular ionic/hydrogen bonding interaction between the Fe-coordinating His¹⁶¹ and the carboxylate of Glu¹⁶⁰. The latter is situated in a loop that

links two Fe-coordinating residues (Asp¹⁵⁷ and His¹⁶¹) in the opposing subunit. The relevance, if any, of structural communication between the active sites to the kinetics and mechanism of these enzymes is not established.

Modelling of the *P. falciparum* mitochondrially targeted FeSOD

The sequence of the major FeSOD is highly conserved in different Plasmodia species (see Additional file 2) and is encoded by a gene on chromosome 8 (PlasmoDB code PF08_0071 [14]) consisting of a single exon. Another gene product (*PfFeSOD2*) with significant sequence homology is located on chromosome 6. This *PfFeSOD2* gene is interrupted with multiple introns. The original gene model (MAL6P1.194 [14]) was revised by a bioinformatic analysis to maximise primary sequence homology to *PfFeSOD*, leading to a gene predicted to consist of nine exons, separated by eight introns with consensus splice donor/acceptor sites (see Additional file 3). Evidence supporting the model was found by *Plasmodium* interspecies conservation of the intron-exon structure, which is a good predictor for small exons [15] and subsequently confirmed by cDNA cloning [16]. A striking feature of the *PfFeSOD2* gene is that it encodes an N-terminal sequence typical of proteins that are targeted to sub-cellular organelles. The first two exons coincide precisely with ele-

**Figure 2**

A) Ribbon representation of *PfFeSOD* polypeptide chain with colour ramping from the amino terminus in red to the carboxyl terminus in magenta. The iron is shown as a red sphere and its coordinating residues His²⁶, His⁷³, Asp¹⁵⁷ and His¹⁶¹ are shown in cylinder representation. **B)** The *PfFeSOD* dimer coloured by subunit with the Fe atoms as mauve spheres and their coordinating residues in cylinder representation. The figures were made using CCP4 mg [39].

ments of the bipartite signal (see Additional file 4) namely a signal sequence and a transit peptide. A GFP-fusion with the signal is directed to the mitochondrion, despite predictions from the sequence that it would be delivered to the apicoplast [16]. However, the gene structure not only hints at its evolution by exon shuffling, but provides the opportunity for alternatively spliced forms [17].

A homology model (see Additional file 1) of the mitochondrially targeted *PfFeSOD2* was derived using the cytosolic *PfFeSOD* structure solved here. The cytosolic *PfFeSOD* is the closest in sequence of any dismutase to the mitochondrial *PfFeSOD* and hence provides the most suitable coordinate set from which to construct a homology model. The model generated has an rms Δ on all C α atoms of 0.36 Å for the 388 matched residues. Unsurprisingly the secondary structure is predicted to be identical to that of the cytosolic FeSOD of *Plasmodium*. It appears that the active site and dimer interface are also well conserved. This is consistent across the Fe/MnSOD enzyme family, which is a highly conserved enzyme class. It remains to be seen if the two superoxide dismutases from *Plasmodium* are indeed structurally and biochemically

equivalent, or whether the mitochondrially targeted SOD has a different turnover/stability that is required for function within a specific environment in the cell.

Discussion

Superoxide dismutases play a crucial role in the chemical protection strategies many cells adopt to counter the considerable threat posed by the superoxide anion radical. Iron-containing superoxide dismutases are essentially confined to prokaryotes, algae, higher plants and certain protozoa [12]. In contrast, the human superoxide dismutases are either Mn- or Cu/Zn-dependent. Thus, selective inhibitors of FeSODs have potential uses in therapy against diseases caused by pathogens. At first sight it would appear difficult to inhibit *PfFeSOD* using classical 'active-site directed' approaches. The substrate-binding site is small, it needs to accommodate just two atoms and the design of selective inhibitors may be hampered by the structural similarity that the iron-containing superoxide dismutases share with the manganese-dependent enzymes. Superoxide is attracted to the active site of dismutases through a funnel, which comprises residues from both subunits in the dimer. The funnel lies at the top of

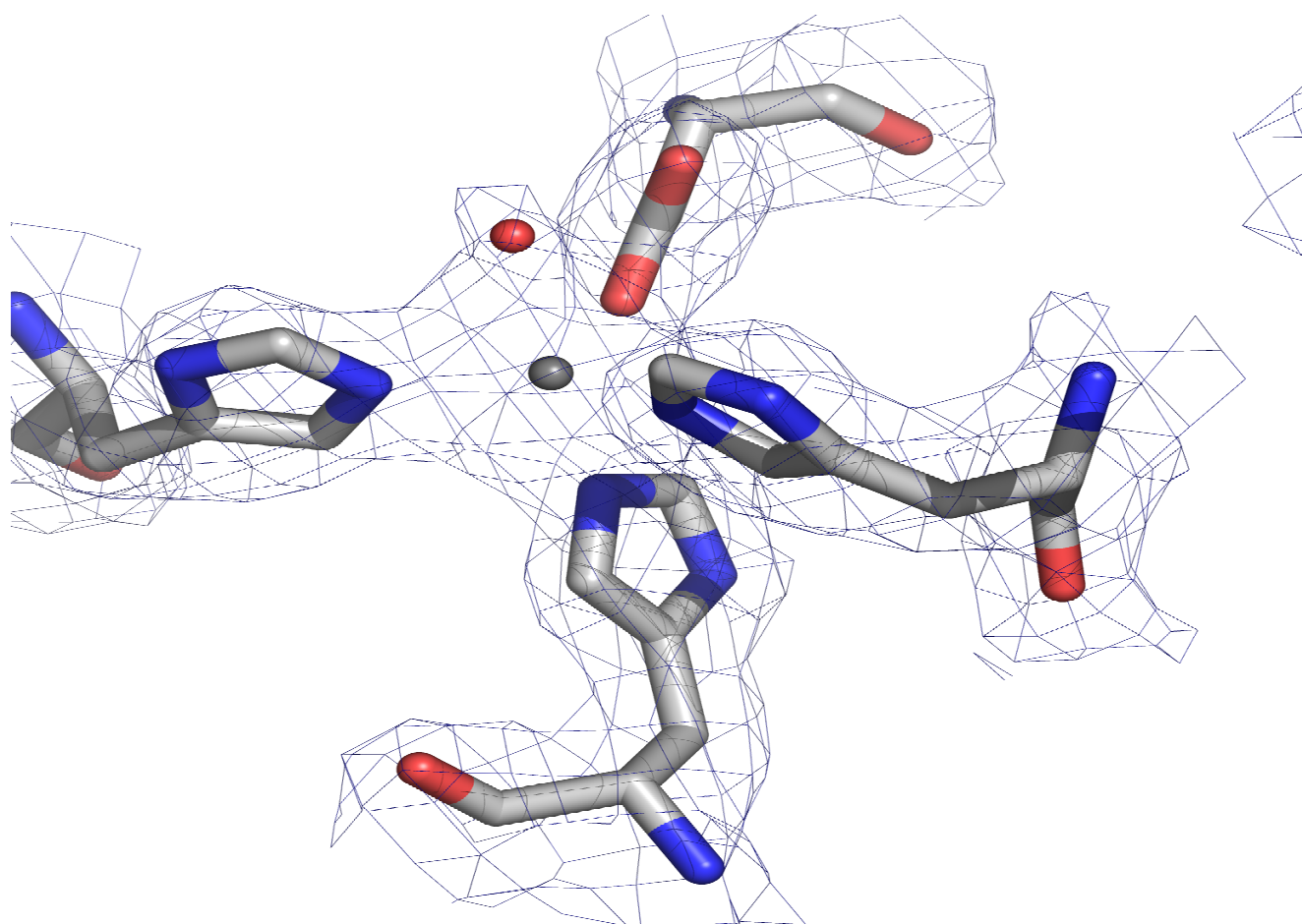


Figure 3

The active site from one subunit of the FeSOD dimer. The metal is shown as a grey sphere and the water molecule that acts as an axial ligand to the metal is coloured red. The $2F_o - F_c$ electron density map, contoured at the one sigma level, is represented as a mesh.

the dimer interface near to the metal sites. It is thought that potential inhibitors could bind here and block access to the active site for the superoxide substrate [13].

An alternative approach is to target inhibitors towards the subunit interface so as to disrupt the quaternary structure. A possible explanation of the widely accepted "ping-pong" kinetics observed for FeSODs would be if superoxide binding in one active site is accompanied by oxidation to oxygen in the other, with the iron atoms in the respective subunits maintaining opposing oxidation states as they alternate between the +2 and +3 forms. If so, dimerisation would likely be important to the mechanism of FeSOD, and monomeric FeSODs are not found in Nature [13]. However, evidence from Cu/ZnSODs suggests that monomeric forms are active which may mean that dimerisation is not crucial for the function of all superoxide dismutases [18]. Despite this, it is clear that the dimer

interface in Fe and MnSODs is important in the SOD reaction with dimer interface mutants of human MnSOD exhibiting reduced steady-state catalytic constants [19,20]. Other evidence points to the importance of dimerisation for functional SOD activity, as dimer destabilising mutations of Cu/Zn SOD have been linked to motor neuron disease [21]. Although the mechanism is unclear, the destabilised mutants may be more prone to aggregation, which is commonly associated with the disease.

There are a number of significant differences between the dimer interfaces in *Pf*FeSOD and HuMnSOD that may be exploited in the design of parasite selective inhibitors. Residue Phe¹¹⁸, which contributes 15 % of the accessible surface area buried in the interface in *Pf*FeSOD is replaced with glutamine in the human enzyme. The intermolecular polar/salt-bridging residue pair of His¹³⁹ and Asp¹⁴⁰ in *Pf*FeSOD is substituted by Cys and Pro, respectively in

HuMnSOD, similarly the Glu²¹-Arg¹⁶⁸ ion pair in *PfFeSOD* appears as Ala and Lys respectively in the human enzyme. These differences ought to be exploitable in the selective design of dimer-disrupting mutants.

Inhibitors of *PfFeSOD* have already been identified from a random screening of a chemical library of compounds [12]. A subset of these uncharged polyaromatic compounds, with molecular weights in the range 200–700 Da, have *in vitro* anti-malarial activity, with IC₅₀ values in the micromolar range. Their mechanism of action and their selectivity was not determined so it remains to be seen whether they interfere with dimer formation. A number of small molecule inhibitors of protein-protein interactions with biomedical significance have been reported recently [22]. For *Trypanosoma cruzi*, a parasite-selective inhibitor of triosephosphate isomerase has been identified and shown to act by blocking dimerisation [23], so it appears that the strategy could be useful, particularly as the percentage of accessible protein surface that becomes buried in a SOD dimer is at the lower limit of the range normally seen in protein multimers in Nature.

Conclusion

The X-ray structure of *P. falciparum* SOD provides the detailed template on which comparisons with human enzyme can be made, and for the design of potential parasite-specific inhibitors. In particular, the biochemical properties of the SOD enzyme (and differences to the human SOD protein) suggest that a possible mode of inhibition would be to disrupt the dimer interface that may be important to its function and stability. The intra-erythrocytic stages of the parasite are in an environment that is known to be rich in antioxidant defences (both chemical and enzymatic) that might compensate an inhibitory effect. However, the selective delivery of inhibitors to the parasite organellar system may prove to be a useful route to new therapeutics.

Methods

Cloning and expression of *P. falciparum* FeSOD

The cytosolic FeSOD coding sequence was amplified from *P. falciparum* (3D7) genomic DNA using Vent™ polymerase (New England Biolabs) and the oligonucleotide primers:

5'-CATGCCATGGTTATTACATTGCCCAAATTAAG-3'

5'-CCGCTCGAGCTTTTGCATAGCTTTTTTAAGTT-3'.

The 597 base pair PCR product was digested with *NcoI* and *XhoI* and ligated to similarly cut pET28a (Novagen). This places the coding sequence for *PfFeSOD* upstream of that for a non-cleavable, C-terminal His₆ tag. The expected expression product therefore comprises residues 1–198 of

PfFeSOD with a C-terminal LEHHHHHH tag. The ligation products were introduced into competent *E. coli* NovaBlue™ cells (Novagen). Kanamycin-resistant transformants harbouring pET28-*PfFeSOD* were identified and isolated. Plasmid DNA from these cells was purified and subsequently introduced into the expression strain *E. coli* BL21-CodonPlus (Stratagene). An overnight culture of *E. coli* BL21/pET28-*PfFeSOD* was used to inoculate 1 litre of Luria-Bertani medium supplemented with 30 µg ml⁻¹ kanamycin and cells were grown with shaking at 37 °C to an OD₆₀₀ of 0.6 at which point expression of recombinant protein was induced by the addition of isopropyl-β, D-thiogalactopyranoside to a final concentration of 1 mM. After a further 4 hours incubation at 30 °C, cells were harvested by centrifugation.

Purification, characterisation and crystallisation

The harvested cell pellet was resuspended in 50 mM Tris-HCl buffer pH 7.5 containing 300 mM NaCl (Buffer A). The cells were lysed by sonication and clarified by centrifugation. The supernatant was mixed with 2 ml Ni-NTA agarose resin (Qiagen) at 4 °C for 1 hour with gentle shaking. The resin was then washed with Buffer A containing 20 mM imidazole and protein was eluted with Buffer A containing 100 mM imidazole. Fractions were examined by Coomassie staining following SDS-polyacrylamide gel electrophoresis and those containing proteins of approximately 23 kDa corresponding to FeSOD were pooled and further fractionated by size exclusion chromatography on a Superdex 75 (Pharmacia) column run in 50 mM Tris-HCl pH 7.5 containing 100 mM NaCl. Typically 10 – 15 mg of protein was obtained per litre of cell culture.

Sedimentation equilibrium experiments were conducted on a Beckman Optima XL/I analytical ultracentrifuge, in an AN-50Ti rotor. The buffer density (300 mM NaCl, 50 mM Tris-HCl, pH 7.5) and the partial specific volume of the protein were estimated to be 1.012 g.ml⁻¹ and 0.7302 respectively, using the program SEDNTERP [24]. Protein homogeneity was examined on an 8.75 % native polyacrylamide gel. Enzyme activity was confirmed using a gel-based Nitro blue tetrazolium assay [25].

Crystallisation experiments were carried out by the hanging-drop vapour-diffusion method. Drops contained a 1:1 volume ratio of *PfSOD* at 10 mg ml⁻¹ in 50 mM Tris-HCl pH 7.5, 100 mM NaCl and a range of precipitants. Rod shaped crystals appeared within a week at 18 °C from reservoir solutions that contained 0.1 M Tris-HCl pH 7.5 and 30–40% (*w/v*) polyethylene glycol (PEG) 600.

Data collection

Crystals were mounted in a fine rayon loop and transferred into a solution containing 0.1 M Tris-HCl (pH 7.5) and 40 % PEG 600 which acts as a cryoprotectant. They

were then flash-cooled in liquid nitrogen. Preliminary in-house X-ray analysis of these crystals showed that they belong to the space group $P2_12_12_1$ with unit cell dimensions $a = 55.5 \text{ \AA}$, $b = 78.4 \text{ \AA}$, $c = 89.3 \text{ \AA}$. A complete X-ray diffraction data set was collected at 100 K, using synchrotron radiation at a wavelength of 0.976 \AA , on beamline ID-29 at the ESRF, Grenoble, using an ADSC Quantum4 CCD detector. The data were processed using the programs *DENZO* and *SCALEPACK* [26].

Structure determination and refinement

Calculations were performed using the *CCP4* suite of programs [27]. Molecular replacement was performed with *AMoRe* [28] and refinement conducted with *REFMAC* [29]. The structure was determined by the molecular replacement method using the *Escherichia coli* FeSOD coordinate set (PDB entry code 1ISC) as a search model. *EcSOD* and *PfSOD* share 51% sequence identity. Molecular replacement calculations produced two clear solutions related by a non-crystallographic 2-fold symmetry axis, and giving an R-factor of 40.4 % after rigid body refinement. Model building was performed using the *X-AUTOFIT* routines [30] implemented in the molecular graphics programme *QUANTA* (Accelrys, San Diego). During refinement, tight non-crystallographic symmetry restraints were imposed on the main chain atoms and medium restraints on the side chains of the two molecules in the dimer.

Modelling the targeted SOD

A homology model of the mitochondrial FeSOD (*PfFeSOD2*) was generated on the basis of 52% sequence identity over 188 residues to the known structure of the cytosolic *PfFeSOD*. All structural visualisation/manipulation was performed using *QUANTA*. The sequences of *PfFeSOD2* and the *PfFeSOD* template structure were aligned using *CLUSTALX* [31], and manually corrected for certain regions, based on interrogation of the known structure.

Homology modelling was performed using *MODELLER6* [32]. Ten initial models were generated, and the model with the lowest objective function chosen as the representative *PfFeSOD2* structure. After manual checking of backbone and side chain positions, energy minimization was performed using *CHARMM* [33,34] to relax steric clashes within the model. Stereochemical evaluation was then performed using *PROCHECK* [35]. The model possesses good stereochemical quality, with 88.4 % of residues in the most favoured regions of the Ramachandran map, and 10.4 % in additional allowed regions. There are four residues in generously allowed or unfavourable regions, which accurately reflect those in the template structure.

Authors' contributions

JAB and IB conceived the study and together with AJW, who coordinated the project, drafted the manuscript; SK provided genomic DNA and advice on cloning; IB expressed the protein with JAB and purified the protein together with CS; IB carried out the crystallographic analysis under the guidance of AMB; DJS carried out the homology modelling work. All authors have approved the final manuscript.

Additional material

Additional File 1

Model of the P. falciparum mitochondrially targeted FeSOD2. Data file PfSOD2_model.pdb.

Click here for file

[<http://www.biomedcentral.com/content/supplementary/1472-6807-6-20-S1.pdb>]

Additional File 2

Sequence alignment of Plasmodia FeSOD sequences. FeSOD is one the most highly conserved proteins across different Plasmodium species [40]. Identical residues are highlighted with a red background and similar residues are boxed. PFeSOD secondary structure elements are superposed. Codes: Pf, P. falciparum; Pr, P. reichenowi; Po, P. ovalae; Pm, P. malariae; Pv, P. vivax; Pk, P. knowlesi; Py, P. yeolii; Pb, P. berghei; Pc, P. chabaudi; Pg, P. gallinaceum. The figure was made using ESPript [38].

Click here for file

[<http://www.biomedcentral.com/content/supplementary/1472-6807-6-20-S2.ppt>]

Additional File 3

Gene model of PFeSOD2. A region of DNA sequence from P. falciparum chromosome 6 is shown, with predicted introns highlighted in yellow, and the protein product of the exon sequences in red.

Click here for file

[<http://www.biomedcentral.com/content/supplementary/1472-6807-6-20-S3.pdf>]

Additional File 4

Sequence alignment of predicted PFeSOD2 proteins from Plasmodium species. Identical residues are highlighted with a red background and similar residues are boxed. PFeSOD2 predicted secondary structure elements are superposed and exon boundaries are marked with a triangle. Note that the first two exons coincide with the putative signal sequence and transit peptide. Sequence data were gleaned from PlasmoDB [14]. Although not shown, the incomplete sequence data from P. chabaudi (missing region around exons 4 & 5) and P. gallinaceum (missing region encompassing 6 & 7) also show the same conserved pattern of putative intron boundaries. Codes: Pf, P. falciparum; Pr, P. reichenowi; Pv, P. vivax; Pk, P. knowlesi; Pb, P. berghei; Py, P. yeolii.

Click here for file

[<http://www.biomedcentral.com/content/supplementary/1472-6807-6-20-S4.ppt>]

Acknowledgements

This work was funded by the Wellcome Trust (Malaria Functional Genomics Initiative, grant no. 066742/F/01/Z). I.W.B. was funded by a BBSRC PhD studentship. The authors wish to thank Andrew Leech (University of York) for AUC analysis, Matt Berriman (Sanger Centre) for bioinformatic insights, and the ESRF, Grenoble for providing excellent data collection facilities.

References

- Beyer W, Imlay J, Fridovich I: **Superoxide dismutases**. *Prog Nucleic Acid Res Mol Biol* 1991, **40**:221-253.
- Fairfield AS, Meshnick SR, Eaton JW: **Malaria parasites adopt host cell superoxide dismutase**. *Science* 1983, **221**(4612):764-766.
- Becuwe P, Gratepanche S, Fourmaux MN, Van Beeumen J, Samyn B, Mercereau-Puijalon O, Touzel JP, Slomianny C, Camus D, Dive D: **Characterization of iron-dependent endogenous superoxide dismutase of Plasmodium falciparum**. *Mol Biochem Parasitol* 1996, **76**(1-2):125-134.
- Bustamante LY, Crooke A, Martinez J, Diez A, Bautista JM: **Dual-function stem molecular beacons to assess mRNA expression in AT-rich transcripts of Plasmodium falciparum**. *Bio-techniques* 2004, **36**(3):488-494.
- Stallings WC, Patridge KA, Strong RK, Ludwig ML: **Manganese and iron superoxide dismutases are structural homologs**. *J Biol Chem* 1984, **259**(17):10695-10699.
- Tainer JA, Getzoff ED, Beem KM, Richardson JS, Richardson DC: **Determination and analysis of the 2 A-structure of copper, zinc superoxide dismutase**. *J Mol Biol* 1982, **160**(2):181-217.
- Parker MW, Blake CC: **Iron- and manganese-containing superoxide dismutases can be distinguished by analysis of their primary structures**. *FEBS Lett* 1988, **229**(2):377-382.
- Misra HP, Fridovich I: **Inhibition of superoxide dismutases by azide**. *Arch Biochem Biophys* 1978, **189**(2):317-322.
- Sugio S, Hiraoka BY, Yamakura F: **Crystal structure of cambialistic superoxide dismutase from porphyromonas gingivalis**. *Eur J Biochem* 2000, **267**(12):3487-3495.
- Gratepanche S, Menage S, Touati D, Wintjens R, Delplace P, Fontecave M, Masset A, Camus D, Dive D: **Biochemical and electron paramagnetic resonance study of the iron superoxide dismutase from Plasmodium falciparum**. *Mol Biochem Parasitol* 2002, **120**(2):237-246.
- Meshnick SR, Kitchener KR, Trang NL: **Trypanosomatid iron-superoxide dismutase inhibitors. Selectivity and mechanism of N1,N6-bis(2,3-dihydroxybenzoyl)-1,6-diaminohexane**. *Biochem Pharmacol* 1985, **34**(17):3147-3152.
- Souler L, Delplace P, Davioud-Charvet E, Py S, Sergheraert C, Perie J, Ricard I, Hoffmann P, Dive D: **Screening of Plasmodium falciparum iron superoxide dismutase inhibitors and accuracy of the SOD-assays**. *Bioorg Med Chem* 2003, **11**(23):4941-4944.
- Munoz IG, Moran JF, Becana M, Montoya G: **The crystal structure of an eukaryotic iron superoxide dismutase suggests intersubunit cooperation during catalysis**. *Protein Sci* 2005, **14**(2):387-394.
- PlasmoDB: The Plasmodium Genome Resource** [<http://www.plasmodb.org>].
- Thompson J, Janse CJ, Waters AP: **Comparative genomics in Plasmodium: a tool for the identification of genes and functional analysis**. *Mol Biochem Parasitol* 2001, **118**(2):147-154.
- Sienkiewicz N, Daher W, Dive D, Wrenger C, Viscogliosi E, Wintjens R, Jouin H, Capron M, Muller S, Khalife J: **Identification of a mitochondrial superoxide dismutase with an unusual targeting sequence in Plasmodium falciparum**. *Mol Biochem Parasitol* 2004, **137**(1):121-132.
- van Lin LH, Pace T, Janse CJ, Birago C, Ramesar J, Picci L, Ponzi M, Waters AP: **Interspecies conservation of gene order and intron-exon structure in a genomic locus of high gene density and complexity in Plasmodium**. *Nucleic Acids Res* 2001, **29**(10):2059-2068.
- Pesce A, Capasso C, Battistoni A, Folcarelli S, Rotilio G, Desideri A, Bolognesi M: **Unique structural features of the monomeric Cu,Zn superoxide dismutase from Escherichia coli, revealed by X-ray crystallography**. *J Mol Biol* 1997, **274**(3):408-420.
- Hearn AS, Fan L, Lepock JR, Luba JP, Greenleaf WB, Cabelli DE, Tainer JA, Nick HS, Silverman DN: **Amino acid substitution at the dimeric interface of human manganese superoxide dismutase**. *J Biol Chem* 2004, **279**(7):5861-5866.
- Ramilo CA, Leveque V, Guan Y, Lepock JR, Tainer JA, Nick HS, Silverman DN: **Interrupting the hydrogen bond network at the active site of human manganese superoxide dismutase**. *J Biol Chem* 1999, **274**(39):27711-27716.
- Hough MA, Grossmann JG, Antonyuk SV, Strange RW, Doucette PA, Rodriguez JA, Whitson LJ, Hart PJ, Hayward LJ, Valentine JS, Hasnain SS: **Dimer destabilization in superoxide dismutase may result in disease-causing properties: structures of motor neuron disease mutants**. *Proc Natl Acad Sci U S A* 2004, **101**(16):5976-5981.
- Arkin MR, Wells JA: **Small-molecule inhibitors of protein-protein interactions: progressing towards the dream**. *Nat Rev Drug Discov* 2004, **3**(4):301-317.
- Tellez-Valencia A, Olivares-Illana V, Hernandez-Santoyo A, Perez-Montfort R, Costas M, Rodriguez-Romero A, Lopez-Calahorra F, Tuena De Gomez-Puyou M, Gomez-Puyou A: **Inactivation of triosephosphate isomerase from Trypanosoma cruzi by an agent that perturbs its dimer interface**. *J Mol Biol* 2004, **341**(5):1355-1365.
- Laue TM, Shah BD, Ridgeway TM, Pelletier SL: **Computer-aided interpretation of analytical sedimentation data for proteins**. In *Analytical Ultracentrifugation in Biochemistry and Polymer Science* Edited by: Harding SE, Rowe AJ, Horton JC. Cambridge, The Royal Society of Chemistry; 1992:90-125.
- Flohe L, Otting F: **Superoxide dismutase assays**. *Methods Enzymol* 1984, **105**:93-104.
- Otwinowski Z, Minor W: **Processing of X-ray diffraction data collected in oscillation mode**. In *Macromolecular Crystallography, Pt A Volume 276*. San Diego, ACADEMIC PRESS INC; 1997:307-326.
- Collaborative Computational Project, Number 4: **The CCP4 Suite - Programs for Protein Crystallography**. *Acta Crystallogr D Biol Crystallogr* 1994, **50**:760-763.
- Navaza J: **Amore - an Automated Package for Molecular Replacement**. *Acta Crystallogr Sect A* 1994, **50**:157-163.
- Murshudov GN, Vagin AA, Dodson EJ: **Refinement of macromolecular structures by the maximum-likelihood method**. *Acta Crystallogr D Biol Crystallogr* 1997, **53**:240-255.
- Oldfield T: **Applications for macromolecular map interpretation: X-AUTOFIT, X-POWERFIT, X-BUILD, X-LIGAND, and X-SOLVE**. *Methods Enzymol* 2003, **374**:271-300.
- Thompson JD, Gibson TJ, Plewniak F, Jeanmougin F, Higgins DG: **The CLUSTAL_X windows interface: flexible strategies for multiple sequence alignment aided by quality analysis tools**. *Nucleic Acids Res* 1997, **25**(24):4876-4882.
- Sali A, Blundell TL: **Comparative protein modelling by satisfaction of spatial restraints**. *J Mol Biol* 1993, **234**(3):779-815.
- Brooks BR, Brucoleri RE, Olafson BD, States DJ, Swaminathan SJ, Karplus M: **CHARMM: a Program for Macromolecular Energy, Minimization and Dynamics Calculations**. *J Comput Chem* 1983, **4**(2):187-217.
- MacKerell AD, Bashford D, Bellott M, Dunbrack RL, Evanseck JD, Field MJ, Fischer S, Gao J, Guo H, Ha S, Joseph-McCarthy D, Kuchnir L, Kuczera K, Lau FTK, Mattos C, Michnick S, Ngo T, Nguyen DT, Prodhom B, Reiher WE, Roux B, Schlenkrich M, Smith JC, Stote R, Straub J, Watanabe M, Wiorkiewicz-Kuczera J, Yin D, Karplus M: **All-atom empirical potential for molecular modeling and dynamics studies of proteins**. *J Phys Chem B* 1998, **102**(18):3586-3616.
- Laskowski RA, MacArthur MW, Moss DS, Thornton JM: **Procheck - a Program to Check the Stereochemical Quality of Protein Structures**. *J Appl Crystallogr* 1993, **26**:283-291.
- Borgstahl GE, Parge HE, Hickey MJ, Beyer WFJ, Hallewell RA, Tainer JA: **The structure of human mitochondrial manganese superoxide dismutase reveals a novel tetrameric interface of two 4-helix bundles**. *Cell* 1992, **71**(1):107-118.
- Wintjens R, Noel C, May AC, Gerbod D, Dufernez F, Capron M, Viscogliosi E, Rooman M: **Specificity and phenetic relationships of iron- and manganese-containing superoxide dismutases on the basis of structure and sequence comparisons**. *J Biol Chem* 2004, **279**(10):9248-9254.

38. Gouet P, Courcelle E, Stuart DI, Metoz F: **ESPrpt: analysis of multiple sequence alignments in PostScript.** *Bioinformatics* 1999, **15(4)**:305-308.
39. Potterton L, McNicholas S, Krissinel E, Gruber J, Cowtan K, Emsley P, Murshudov GN, Cohen S, Perrakis A, Noble M: **Developments in the CCP4 molecular-graphics project.** *Acta Crystallogr D Biol Crystallogr* 2004, **60(Pt 12 Pt 1)**:2288-2294.
40. Baert CB, Deloron P, Viscogliosi E, Delgado-Viscogliosi P, Camus D, Dive D: **Cloning and characterization of iron-containing superoxide dismutase from the human malaria species *Plasmodium ovale*, *P. malariae* and *P. vivax*.** *Parasitol Res* 1999, **85(12)**:1018-1024.

Publish with **BioMed Central** and every scientist can read your work free of charge

"BioMed Central will be the most significant development for disseminating the results of biomedical research in our lifetime."

Sir Paul Nurse, Cancer Research UK

Your research papers will be:

- available free of charge to the entire biomedical community
- peer reviewed and published immediately upon acceptance
- cited in PubMed and archived on PubMed Central
- yours — you keep the copyright

Submit your manuscript here:
http://www.biomedcentral.com/info/publishing_adv.asp

